STUDY OF CLOSED DIVERTOR WITH STRONG GAS-PUFFING ON THE JFT-2M

H. KAWASHIMA, S. SENGOKU, T. OGAWA, H. OGAWA, K. UEHARA,
Y. MIURA, H. KIMURA and the JFT-2M Team
Naka Fusion Research Establishment, Japan Atomic Energy Research Institute,
Tokai Annex, 2-4 Tokai-mura, Naka-gun, Ibaraki-ken, 319-1195 Japan

Abstract

In order to improve the particle control capability of the divertor and to demonstrate the possibility of a dense and cold divertor with high confinement plasmas, a closed divertor study has been carried out on the JFT-2M tokamak. When a strong gas-puff is applied into the divertor chamber, a baffling effect is exhibited by enhanced radiation localization and high neutral pressure in the divertor chamber, low core fueling and sustainment of core confinement quality. The baffling effect is further enhanced with ExB flow and/or current in the scrape off layer induced by divertor biasing. A dense and cold divertor state (n_e^{div}~$4x10^{19}m^{-3}$ and T_e^{div}~4eV) by strong gas-puffing can be obtained together with the improved confinement modes. Furthermore, the improved core confinement is not affected significantly in the high density region ($\overline{n_e}/n_e^G < 0.7$). The UEDA-code simulation reproduces the baffling effect and a dense and cold divertor plasma with a closed divertor structure.

1. INTRODUCTION

The divertor of a fusion reactor must be designed to minimize the heat load to the divertor targets and to ensure sufficiently low neutral density in the main plasma periphery, so that the confinement is not degraded. However, the quality of core plasma confinement in the present tokamaks is adversely affected by fuel or impurity gas-puffing in the divertor region [1]. If the radiation from fuel atoms or impurities can be largely localized in the divertor region, the degradation of energy confinement due to the radiation can be prevented. The possible confinement deterioration by neutrals in the main chamber leads to the development of a closed divertor structure that can retain neutrals in the divertor chamber. Some tokamak machines, therefore, have been modified to a closed divertor structure [2].

A study on the closed divertor has also been carried out in JFT-2M with the aim of making a dense and cold divertor, compatible with high core confinement (e.g. H-mode). The lower inside of the JFT-2M vacuum vessel was modified to a closed divertor configuration in 1995 in order to control the divertor plasmas and neutrals independently from the core plasmas. At first, the divertor structure was a less closed configuration the effect of which was not sufficient to achieve the purpose [3]. Up to now, the degree of closure (defined later) has been improved from 1.3 to 0.8, which is the most closed configuration compared with other machines [4].

This paper describes experimental results with this configuration. In section 2, the structure of the JFT-2M closed divertor is presented. In sections 3 and 4 respectively, the baffling effect and the effect of strong gas-puffing on improved confinement modes are presented. The baffling effect is confirmed by the localized radiation and high neutral pressure in the divertor region, lower core fueling and sustainment of good core confinement. The baffling effect is enhanced significantly with ExB flow and/or current in the scrape off layer (SOL) by applying negative biasing to both inner and outer divertor plates. Not only can a typical dense and cold divertor state be obtained by a strong gas-puff in the divertor chamber, but also improved core confinement is kept almost constant in the high density region. The result of UEDA-code simulation [5] is presented in section 5. It shows the effect of the closed divertor configuration on neutral density and on electron density and temperature in the divertor chamber. Finally, conclusions are given in section 6.

2. CLOSED DIVERTOR AND EXPERIMENTAL SETUP

Figure 1 shows a schematic view of the closed divertor in the lower part of the JFT-2M vacuum vessel. The baffle plates are set inside, outside and at private regions in the divertor chamber to shield the core plasma from neutral back-flow and to increase the divertor neutral pressure. The divertor and baffle plates are made from stainless steel. Up to now, the degree of closure, which is defined as $\delta / \lambda_{1/e}$, where δ is the width of the divertor throat and $\lambda_{1/e}$ is the e-folding length of particle flux, has been changed from 1.3 to 0.8. A lower single null divertor configuration (LSN) is used for the closed divertor. The upper part still has an open structure and upper single null (USN) discharges are used as a reference to the closed divertor. Graphite plates are used in the upper divertor. A deuterium gas-puff is applied to each divertor region at LSN or USN. Some diagnostic systems are installed in the divertor region. The electron temperature and density on the divertor and baffle plates are measured by a Langmuir probe array with high spatial resolution (5~20mm). The neutral gas pressure is measured by Penning gauges. A bolometer is used to measure the total radiation loss from the main plasma. Three bolometer array systems are also used to measure the radiation profiles horizontally and vertically in the main plasma region, and the profile at the outer divertor leg. The soft x-ray emission profile is also measured by a radial array of PIN diodes at the top.

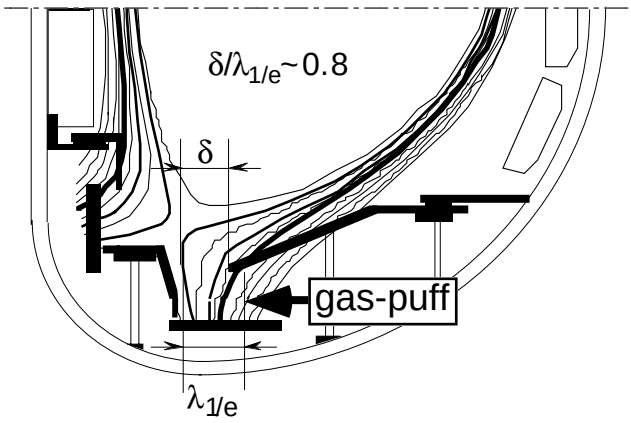

FIG.1 Schematic view of JFT-2M closed divertor. δ is the width of the divertor throat and $\lambda_{1/e}$ is the e-folding length of particle flux.

The major and minor radii in discharges described hereafter are around 1.3m and 0.26m, and the elongation factor is 1.5. The toroidal field and plasma current are ~1.3T and ~230kA. The surface safety factor is 3~4. The line averaged electron density ($\overline{n_e}$) of the target plasma is 1.5-3.5x$10^{19}$$m^{-3}$. The hydrogen neutral beam power (P_{NBI}) is 0.3~0.8MW. Deuterium is used as the working gas.

3. BAFFLING EFFECT OF THE CLOSED DIVERTOR CONFIGURATION

In order to investigate the baffling effect of the closed divertor, the plasma performance is compared between the LSN (closed) and USN (open) divertor configurations. A strong gas-puff is applied into the divertor chamber to enhance the remote radiative cooling. Figure 2(a) shows the time evolution of plasma parameters with application of a divertor gas-puff (Q_{div}) of 3.0Pam^3/s, which is several times larger than that of the normal operation, during neutral beam heated (P_{NBI}=0.6MW) L-mode. Solid and broken lines show the cases of LSN and USN, respectively. The increase in P_{rad}^{mid} and D_α light and the decrease in peripheral electron temperature and energy confinement time are smaller for LSN than for USN. The increment of $\overline{n_e}$ for LSN is 70~80% of that for USN and P_0^{div} increases from ~20mPa to ~100mPa for LSN. Figure 2(c) shows the horizontal radiation profiles (the viewing chord of each channel is shown in Fig.2(b)) in both LSN and USN cases. The bolometers of ch.8~ ch.13 are viewing the lower closed divertor region for the case of LSN, those of ch.23~ch.26 are viewing the open divertor region for the case of USN and those of ch.16~ch.22 are viewing the main plasma region. The enhancement of the radiation loss from t=0.7s to 0.8s is indicated by the shading in the figure. The radiation

loss is enhanced entirely from the divertor to the main plasma regions for the USN case. For the LSN case, the radiation loss is enhanced only in the divertor region and is rather reduced a little in the main plasma region. It might be expected that radiation enhancement in the main plasma region caused the confinement degradation in the USN case. In contrast, the confinement may not be degraded in the LSN case since the radiation enhancement is localized only in the divertor region. It is suggested that the baffle plates are effective for making radiation localized in the divertor, high divertor neutral pressure and low core fueling.

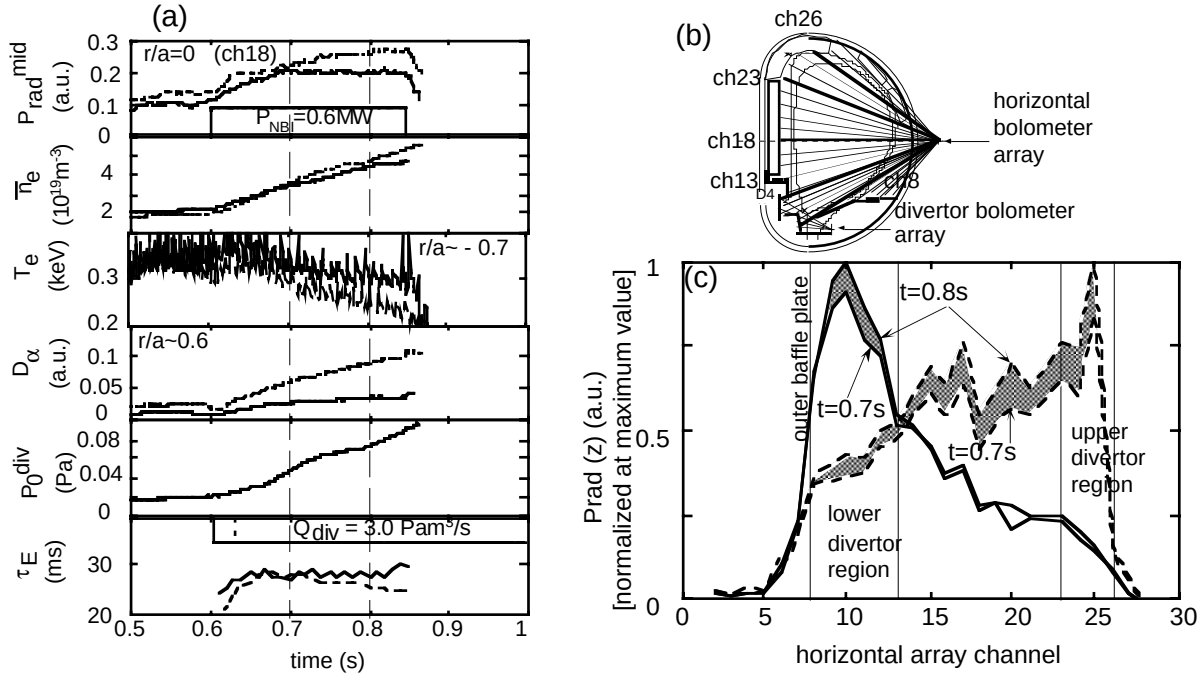

FIG.2 (a)Time evolution of radiation loss at the center chord P_{rad}^{mid}, line averaged electron density at the center chord $\bar{n}_e$, electron temperature at r/a~ -0.7, D_α light through r/a~0.6, neutral pressure of the divertor chamber P_o^{div} and energy confinement time τ_E with a gas-puff of 3.0 Pam³/s in L-mode discharges with LSN(solid line) and USN (broken line). (b) Viewing chords of horizontal and divertor bolometer array systems, and (c) horizontal radiation profiles at t=0.7s and 0.8s for LSN and USN.

The enhancement of the baffling effect is observed with divertor biasing [6]. When both inner and outer divertor plates are negatively biased with respect to the vacuum vessel, a significant difference in the plasma parameters is observed. Figure 3 shows the time evolution in such discharges. Solid and broken lines show cases with and without biasing, respectively. $\overline{n_e}$, P_{rad}^{total} and D_α are reduced by 20% , 40% and 30%, respectively. And an increase in P_0^{div} by a factor of ~1.5 is observed at a bias voltage of -150V. Figures 3(b) and 3(c) show the horizontal and divertor radiation profiles at t=0.725s. The viewing chords of the four channel divertor bolometer array are also shown in Fig.2(b). The horizontal profile shows a reduction by 50~75% for all the channels by biasing. But the radiation power of the outer divertor leg increases to ~1.6 times as shown by the divertor profiles. Since a negative radial electric field is formed in the SOL by biasing [7], the ExB flow from inside to outside is formed in the SOL. The SOL current is also observed from inside to outside divertor in this case. Thus the ExB flow and/or current in the SOL increases the baffling effect and enhances radiation in the divertor chamber dramatically.

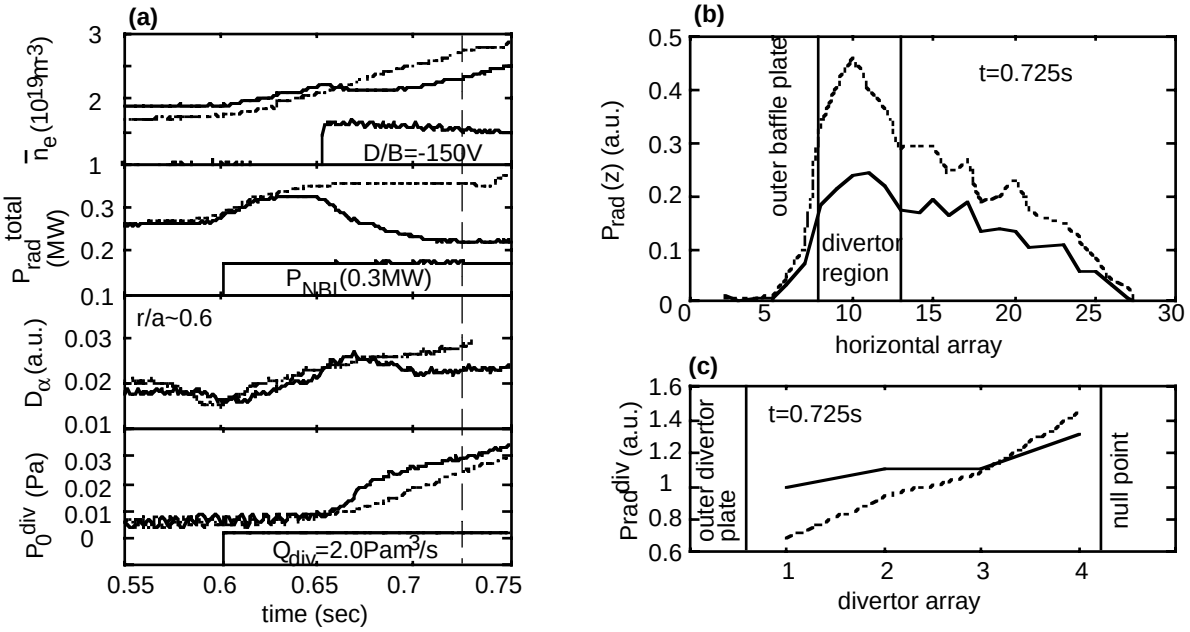

FIG.3. (a)Time evolution of $\overline{n}_e$, total radiation P_{rad}^{total}, D_α and P_0^{div} with negative biasing of both inside and outside divertor plates (solid line) in the case of an L-mode discharge with gas-puffing (ccw B_T). Broken line shows a case without biasing. (b) and (c) show the radiation profiles at t=0.725s measured by horizontal and divertor bolometer arrays , respectively .

4. EFFECT OF A STRONG GAS-PUFF ON CORE CONFINEMENT AND DENSE AND COLD DIVERTOR

The main purpose of the closed divertor study on JFT-2M is to obtain dense and cold divertor plasmas by gas-puffing during H-mode and to avoid core confinement degradation by independent control of divertor and main plasmas. Using the present most closed structure, we have obtained the result that, under optimum conditions of null point, plasma location, and safety factor, the dense and cold divertor state can be demonstrated with strong gas-puffing and the ELM free H-mode can be maintained for a longer time at low target densities around $2\times10^{19}m^{-3}$ [8]. With the open divertor of USN, the duration of the H-mode was shortened by gas-puffing and the dense and cold divertor could not progress during the H-mode.

Two types of improved confinement modes are obtained with the dense and cold divertor state after H-mode at high target densities over $3\times10^{19}m^{-3}$. One is IL-mode(type I) which holds a radiation level and a high stored energy constantly probably due to the appearance of sawteeth. This mode occurs after ELM free H-mode with continuous gas-puffing. The other is IL-mode(type II) which is similar to the IL-mode first obtained in 1988 on the JFT-2M open divertor [9]. IL-mode(type I) and (type II) are distinguished by whether the sawtooth oscillation appears or not.

Figure 4(a) shows a typical time evolution indicating a transition from H-mode to the IL-mode(type I). The neutral beam (P_{NBI}=0.8MW) is injected from t=0.6s and Q_{div} (3.0 to 2.0Pam^3/s) is applied during the beam pulse. An ELM free H-mode transition took place at the density of $\sim3\times10^{19}m^{-3}$ at t=0.64s. The P_{rad}^{total} decreases just after the H-mode transition and then increases abruptly. W_s and $\overline{n_e}$ increase to 29kJ and $5\times10^{19}m^{-3}$, respectively. After the H-mode is terminated at t=0.68s, the discharge undergoes the second transition from H-mode to IL-mode(type I), where P_{rad}^{total} and W_s (~33kJ) are kept constantly high by the end of the neutral beam pulse and $\overline{n_e}$ increases gradually and reaches a maximum density of $\sim7\times10^{19}m^{-3}$.

Simultaneously, divertor plasmas progress to a dense and cold state of $n_e^{div}>2x10^{19}m^{-3}$ and T_e^{div} <10eV. In this mode, the sawtooth oscillation becomes remarkable and the short period H-mode transition is repeated at each oscillation. The broadening and peaking of soft x-ray profiles are repeated for short H- and L-modes of the sawtooth interval as shown in Fig.4(b). As a result, the global parameters of the radiation and the stored energy are kept constantly high. This mode can be obtained by decreasing gas-puffing from 3.0 to 2.0Pam^3/s at t=0.73s. If Q_{div}=3.0Pam^3/s is applied continuously at the end of the neutral beam pulse, the stored energy decreases at a later period. If the gas-puffing is turned off from t=0.73s, the discharge is not steady, such that the radiation and stored energy are changed greatly at each sawtooth period. This mode depends significantly on the amount of gas-puffing.

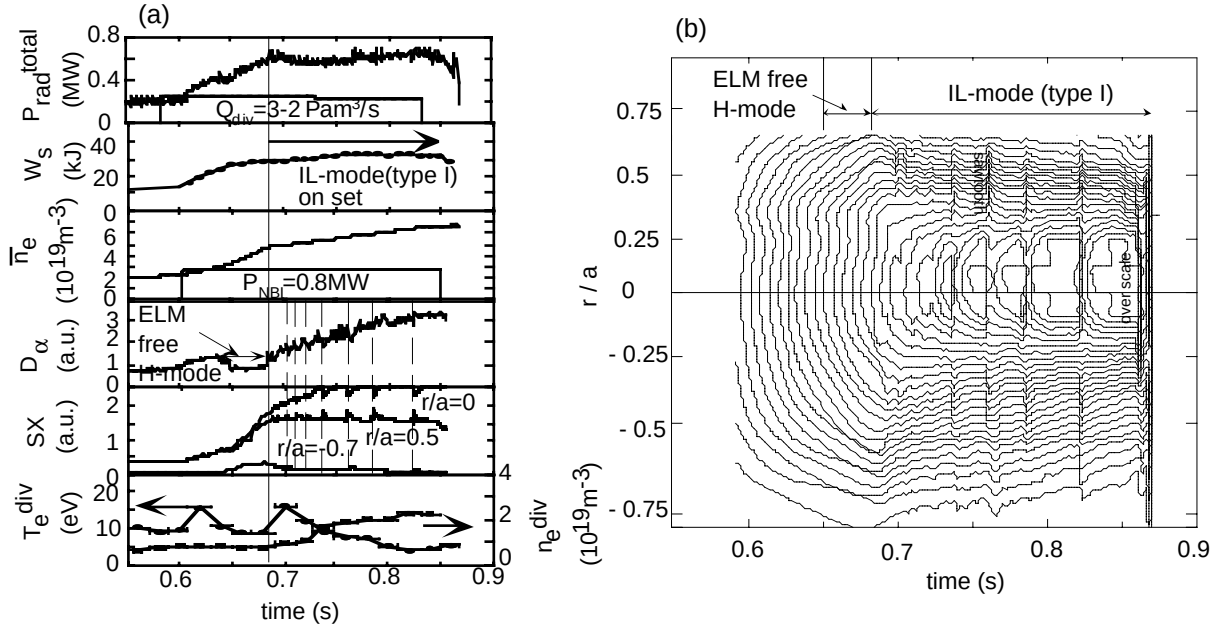

*FIG. 4. Time evolution of (a): plasma parameters in the **IL-mode(type I)** obtained with strong gas-puffing during ELM free H-mode and (b):contour lines of the soft x-ray profile. Here, W_s, SX, T_e^{div} and n_e^{div} are the stored energy, soft x-ray emission, divertor electron temperature and density, respectively.*

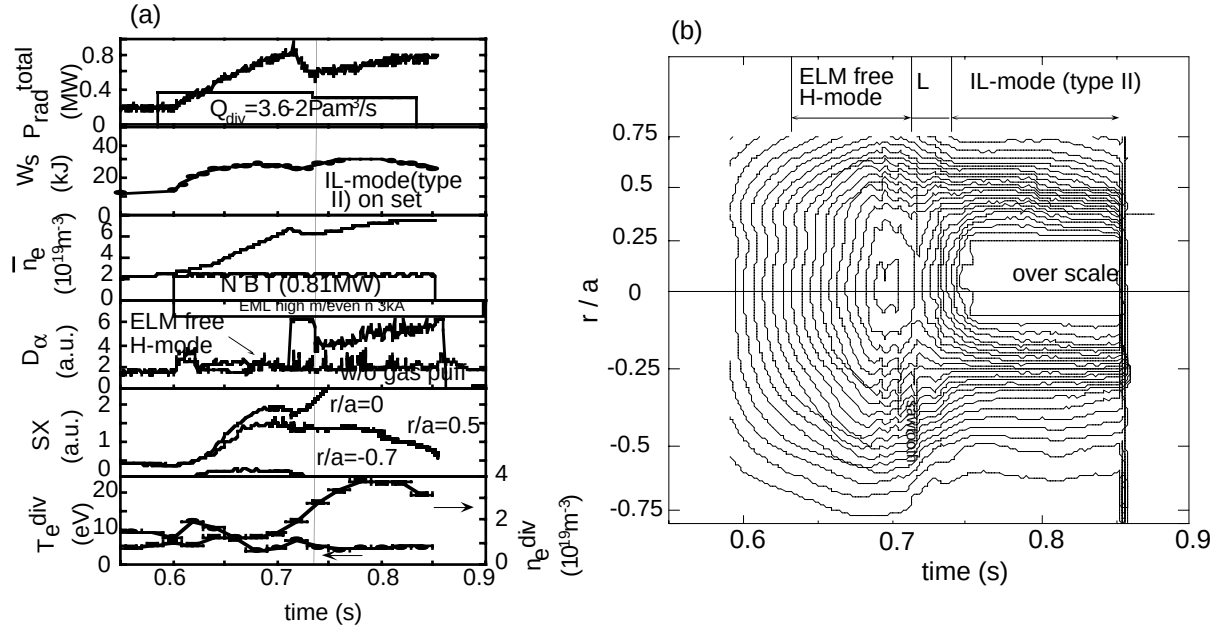

*FIG.5. Time evolution of (a): plasma parameters in the **IL-mode (type II)** obtained with strong gas-puffing during an ELMy H-mode which is produced by applying the ergodic magnetic field and (b): contour lines of the soft x-ray profile.*

On the other hand, when the ergodic magnetic structure was applied with the EML (Ergodic Magnetic Limiter) coil, after a short ELM free H-mode, ELMy H-mode could be created without gas-puffing as shown by the D_α signal in Fig.5(a) [10]. By applying a gas-puff of Q_{div}=3.6Pam^3/s in this discharge, the ELM free H-mode is prolonged for ~90ms. The P_{rad}^{total} and $\overline{n_e}$ increase abruptly, and W_s also increases to 27kJ in this period. The ELM does not appear after the ELM free H-mode termination. The H/L transition occurs at t=0.71s as seen with the abrupt jump in D_α, and P_{rad}^{total}, $\overline{n_e}$ and W_s decrease. Then an IL-mode (type II) transition occurs at t=0.74s, where D_α decreases and P_{rad}^{total}, $\overline{n_e}$ and W_s increase again accompanied by a remarkable dense and cold divertor (n_e^{div}~4x10^{19}m^{-3} and T_e^{div}~4eV). W_s reaches ~31kJ, higher than the value during H-mode. However, it decreases with increasing radiation loss later. As shown in the soft x-ray profile during the IL-mode (type II) (Fig.5(b)), the sawtooth oscillation disappears and the profiles around the center (-0.3< r/a < 0.5) are peaked dramatically. In contrast, the peripheral region is broadened. It seems that the energy and particle confinement around the plasma core is improved, while the confinement in the peripheral region is worse. The reason is not fully understood yet, but there is a possibility of enhanced diffusion in the peripheral stochastic magnetic layer by EML or the effect on edge transport of the high recycling conditions. The IL-mode (type II) is quite similar to the previous IL-mode. But there is a difference the radiation loss in the divertor regions. For the previous IL-mode, the radiation is reduced to ~2/3 compared with that during H-mode. The radiation in the divertor is enhanced by 1.7 times over that of the H-mode and a remarkable dense and cold divertor state is developed for this IL-mode (type II).

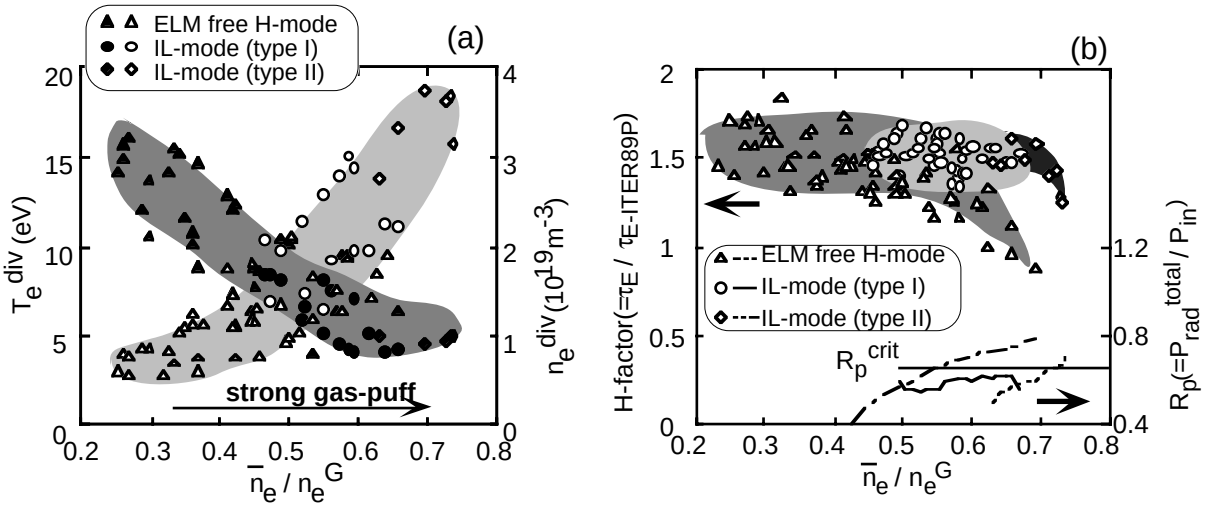

FIG.6 (a): Progress of the dense and cold divertor and (b): characteristics of main plasma confinement in the ELM free H-mode, IL-mode (type I) and IL-mode (type II), when the main plasma density normalized by the Greenwald density limit n_e^G is increased by gas-puffing in the closed divertor chamber. The $\overline{n_e}/n_e^G$ dependence of Rp(ratio of P_{rad}^{total} to input power P_{in}) in a discharge which reaches the highest density of each mode is also shown in (b).

Thus, the dense and cold divertor together with improved confinement discharges of the ELM free H-mode, IL-mode (type I) and IL-mode (type II) can be obtained by strong gas-puffing in the divertor chamber. In Fig. 6(a) and (b), the divertor electron temperature and density and the enhancement factor (H-factor) of the global energy confinement time are summarized as a function of the main plasma density normalized by the Greenwald density limit. All discharges in Fig.6 have an attached divertor condition, i.e. the detachment is hardly observed, which will be discussed elsewhere. When $\overline{n_e}/n_e^G$ is increased by gas-puffing, T_e^{div} is decreased linearly, and then saturates at ~4eV around $\overline{n_e}/n_e^G$=0.6. n_e^{div} is not changed so much in low density regions ($\overline{n_e}/n_e^G$<0.4) and increases quickly from $\overline{n_e}/n_e^G$~0.4 when T_e^{div} becomes less than 10eV. The

ionization of deuterium neutrals and the electron energy loss may be enhanced. The H-factor is kept nearly constant (~1.5) up to $\overline{n_e}/n_e^G$=0.6 with the ELM free H-mode and $\overline{n_e}/n_e^G$ =0.7 in IL-mode (type I) and IL-mode(type II). Strong degradation of the H-factor with increasing density, which is observed in other divertor machines, is not observed. However, the H-factor of ELM free H-mode and IL-mode (type-II) only degrades at their highest densities corresponding to an abrupt increase in radiation loss over the critical value of R_p^{crit}~0.7 in the main plasma as shown in Fig.6(b). On the other hand, the radiation loss power for the IL-mode (type I) does not reach to R_p^{crit} , above which the confinement degrades. There is no apparent dependence of the core plasma confinement on the effect of neutrals with strong gas-puffing in the divertor chamber, but it is suggested that the core confinement degradation at the ELM free H-mode and IL-mode (type II) depends strongly on the increase of the core radiation by impurity accumulation. In this sense, the IL-mode (type-I) has superior characteristics for realizing steady-state high performance at high density.

5. UEDA-CODE SIMULATION

UEDA-code, a two dimensional fluid code for divertor simulations coupled with a Monte Carlo method for neutral gas behavior, is applied to JFT-2M divertor configurations with and without the baffle plates. A simulation is carried out for neutral beam heated and high recycle plasmas in which a total loss power to the SOL of 1MW and an edge density of $2x10^{19}m^{-3}$ are assumed. For the particle diffusion coefficient (D) and the thermal diffusivity of electrons and ions ($\chi_{e,i}$), the following values are used : $D=2/3m^2/s$, $\chi_e=2m^2/s$ and $\chi_i=2/3m^2/s$, which is based on the value obtained experimentally [11] and is consistent with the value of the Bohm diffusion coefficient. The buildup of neutral particles and the dense and cold divertor state are compared with their configurations. Figure 7(a) shows the contour plot of neutral density (n_0) in the divertor chamber. The regions over $n_0=5x10^{17}m^{-3}$ in the divertor chamber are indicated by the shading in the figure. It shows that the baffle plates form a steep n_0 gradient in the divertor chamber and increase n_0 to a high density in front of the divertor plates. Figure 7(b) shows poloidal profiles of peak electron temperature ($T_{e\text{-}peak}^C$) and density ($n_{e\text{-}peak}^C$) from the outer to

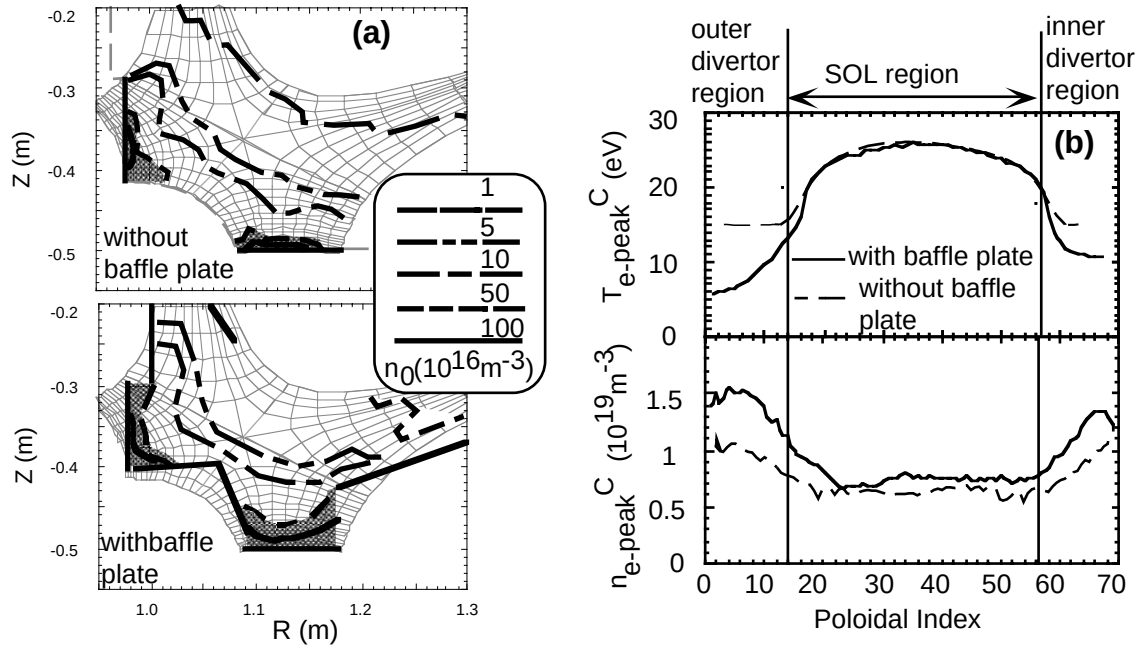

FIG.7 UEDA-code simulation for JFT-2M divertor configurations with and without baffle plates. (a) Contour plot of neutral density n0 in the divertor region. (b) Poloidal profiles of electron temperature and density in the SOL.

the inner divertor through the SOL regions, where the broken and solid lines correspond to the cases with and without the baffle plates. In front of the divertor plate, $T_{e\text{-}peak}{}^{C}$ and $n_{e\text{-}peak}{}^{C}$ reach 5.5eV and $1.5\text{x}10^{19}\text{m}^{-3}$ in the case with baffle plates. This dense and cold state is stronger than in the case without the baffles as shown in the figure, whereas the two cases are almost the same in the SOL region. These simulation results indicate that the neutral buildup and the dense and cold state in the divertor chamber are enhanced in the case of the closed divertor structure with the baffle plates.

6. CONCLUSION

The plasma performance associated with a strong gas-puff into the divertor chamber is compared for open and closed divertor configurations. The baffling effect of the closed configuration is revealed by enhanced radiation loss localization and high neutral pressure (~100mPa) in the divertor regions, lower core fueling (70~80% of that with the open configuration) and the sustainment of energy confinement quality. The baffling effect is also enhanced significantly with ExB flow and/or current in the SOL by applying divertor biasing. Furthermore, a dense and cold divertor up to $n_e{}^{div}$~$4\text{x}10^{19}\text{m}^{-3}$ and $T_e{}^{div}$~4eV together with the improved confinement modes up to $\overline{n_e}/n_e{}^{G}$~0.7 can be brought about by strong gas-puffing. The strong gas-puffing to an ELM free H-mode plasma leads to the second transition to IL-mode (type I), which has favorable features for realizing steady-state high performance at high density. The UEDA-code simulations show that the baffle plates produce a strong neutral buildup and the dense and cold state in the divertor chamber.

ACKNOWLEDGMENT

The authors would like to thank Drs. H.Kishimoto, M.Ohta, A.Funahashi, M.Azumi and M.Shimizu for their support and encouragement.

DEDICATION

The authors dedicate this paper to the memory of Dr. Norio Suzuki, who was the leader of the JFT-2M group and passed away on 11 March 1998. He devoted his life to research on plasma physics and thermonuclear fusion.

REFERENCES

[1] e.g. G. VLASES, et al., in Plasma Physics and Controlled Nuclear Fusion Research 1996 (Proc. 16th Int. Conf. Montreal,1996), Vol. 1, IAEA Vienna (1997) 371 and N. ASAKURA, et al., Plasma Phys. Control. Fusion 39 (1997) 1295.
[2] ITER Physics Basis, to be published in Nuclear Fusion (1998).
[3] S.SENGOKU, et al., Bull. Amer. Phys. Soc. 40 (1995)1675.
[4] S.SENGOKU, et al., Bull. Amer. Phys. Soc. 42 (1997)1962.
[5] N.UEDA. et al., Nucl. Fusion 28 (1988) 118.
[6] H.OGAWA, et al., 13th PSI Conference, San Diego, 1998 (to appear in J. Nucl. Mater).
[7] S. OHDACHI, et al., Plasma Phys. Control. Fusion 36 (1994) A201 and T.SHOJI, et al., in Plasma Physics and Controlled Nucl. Fusion Res. (Proc. 14th Int. Conf. Wurzburg, 1992) Vol. 1 (IAEA, Vienna, 1993)323.
[8] H.KAWASHIMA, et al., Proc 24th Europ. Conf. on Contr. Fusion and Plasma Phys, Berchtesgaden, 21A-II (1997) 705.
[9] M.MORI, et al., Nuclear Fusion 28 (1988) 1892.
[10] H.TAMAI, et al., in Plasma Physics and Controlled Nuclear Fusion Research 1994 (Proc. 15th Int. Conf. Seville,1994), Vol. 1, IAEA Vienna (1995) 371.
[11] K.NAGASHIMA, et al., J. Nucl. Mater. 220-222 (1995) 208.